Wisconsin
Indiana
Yale
NOAO

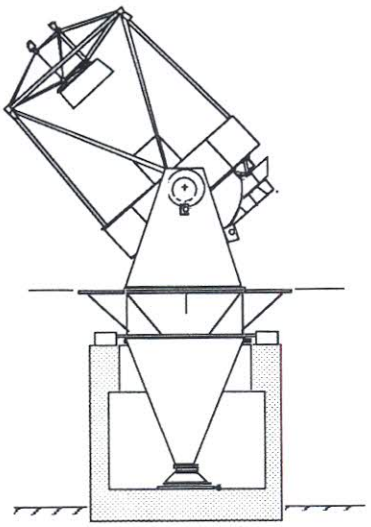

3.5 Meter Telescope

Active Optics System for a 3.5-Meter Structured Mirror

L. Stepp, N. Roddier, D. Dryden

WODC 02-14-01

Presented at SPIE

Active optics system for a 3.5-meter structured mirror

Larry Stepp, Nicolas Roddier, Dave Dryden

National Optical Astronomy Observatories††
P.O. Box 26732, Tucson, Arizona 85726-6732

Myung Cho

Optical Sciences Center, University of Arizona
Tucson, Arizona 85721

ABSTRACT

An active optics system for a 3.5-meter f/1.75 borosilicate honeycomb mirror has been designed and built. The system hardware and software are described, and preliminary test results are presented that demonstrate the structured mirror responds well to the active optics control. Plans for extensive further testing are described. The results of the testing will guide a redesign of the system, before installation of the second-generation system in the WIYN Telescope, to be built on Kitt Peak in Arizona.

1. INTRODUCTION

At six o'clock in the morning of Saint Patrick's day, 1989, a truck started slowly rolling north on Cherry Street in Tucson, under the orange glow of low-pressure sodium street lights. On the bed of the truck was a large shipping container, and inside was a 3.5-meter mirror blank that had been cast the previous December at the Steward Observatory Mirror Laboratory under the University of Arizona football stadium. When the truck arrived at the National Optical Astronomy Observatories headquarters building after a trip of less than a kilometer, the NOAO 3.5-meter Mirror Project began in earnest.

This project has been described in a previous paper. [1] Its principal goal is to develop technology to make possible the construction of high-resolution telescopes of the 8-meter class using structured borosilicate glass mirrors. After completion of the project, the finished 3.5-meter mirror will be installed in the WIYN Telescope on Kitt Peak. [2]

We are presently involved in the second phase of the project, an extensive series of tests to evaluate the performance of the mirror and its associated hardware. One part of this test program is evaluation of the active optics system that was developed for this mirror.

The advantages of active optics for astronomical telescopes have been well described by other authors. [3,4] Our goals for this project are to develop a system that will: 1) allow a relaxation of the polishing tolerances for low-spatial-frequency aberrations, 2) correct figure errors in the telescope caused by performance variations in the support or thermal control systems, 3) allow partial compensation of figure errors in other optical elements. In contrast to some other active optics systems, we are not attempting to actively counter wind loading on the mirror. The distributed defining feature of the axial support design will react wind loads passively without producing large mirror distortions.

---

††Operated by the Association of Universities for Research in Astronomy, Inc. under cooperative agreement with the National Science Foundation.

2. THEORETICAL BACKGROUND

The 3.5-meter active system is similar to an experimental system built previously at NOAO for a 1.8-meter borosilicate honeycomb mirror.[5] However, the current system is different in some respects both in hardware and in its approach to the active control. In setting up the previous system, finite-element analyses were used to calculate the response of the mirror to unit force loads. The influence function from each unit load was fit to a Zernike polynomial, and the coefficients of 36 low order terms were calculated. These sets of coefficients were combined into an influence matrix. This matrix was used to precalculate the force sets, or vectors, required to produce a set of orthogonal displacement modes, in this case individual terms from the Zernike polynomial, using a least-squares fit to calculate the forces required to produce each mode. These force vectors were combined into a matrix that was the pseudo-inverse of the influence matrix.

To correct a measured mirror distortion, the distorted surface was described in terms of Zernike coefficients, and this vector of coefficients was multiplied by the pseudo-inverse matrix to yield a set of forces. This set was the summation of the force sets required to correct the individual Zernike terms in the distorted mirror surface.

On the 3.5-meter mirror a slightly different approach is being applied. As in the previous system, finite-element analyses were performed to calculate the surface distortion of the 3.5-meter WIYN primary mirror subjected to unit forces at the actuator locations. The SAP IV program was used. The finite-element model is a symmetric half-mirror model with 14 element groups and three levels of nodal points (a total of 994 nodes). This model is illustrated in Figure 1. Constant strain plate bending elements were used for the mirror blank and linear translation boundary elements were employed to monitor the reactions at three hard points. These hard points were used for the analysis only, and do not physically exist. Their influence was eliminated by superimposing individual load cases in the correct proportions when creating the influence matrix, so that in each combined case the summation of force at each hard point was zero.

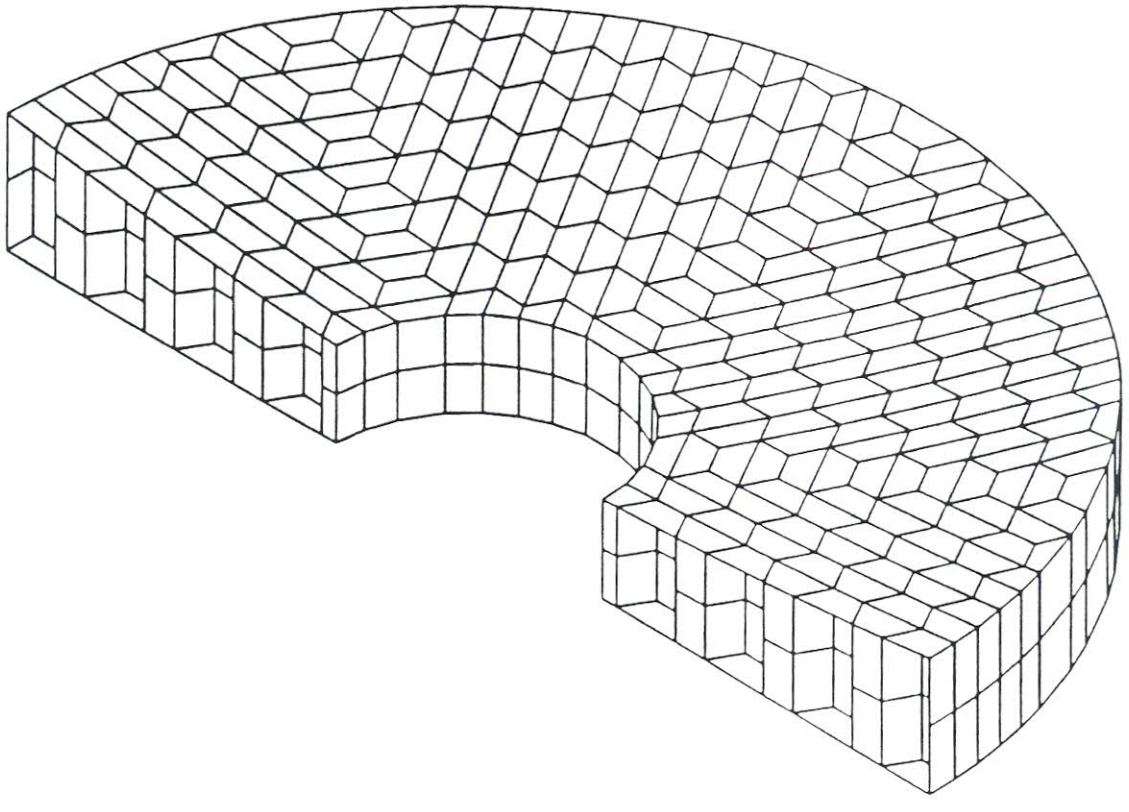

Figure 1. The half-mirror finite-element model.

Thirty-five individual unit load cases were analyzed with the half model; employing symmetry these load cases were sufficient to model the full mirror with a total of 66 actuators. The axial support system is a hydraulic whiffletree, therefore when a force is added at a single support it also produces reactions at the other 65 support locations. To model this effect, the individual unit load cases were superimposed into combined cases, each with 66 different force inputs. The optical surface distortion for each combined case was described by the surface displacements at 292 points on a 20 by 20 square grid. We believe this method of describing the influence functions will introduce smaller errors than fitting to a limited set of Zernike terms. These displacement sets were combined into an influence matrix, with each column in the matrix consisting of the 292 displacements from a single combined case.

The advantages of modal precalculation have been explained by Wilson et al. [6] The calculation of forces can be faster if it requires only a matrix multiplication instead of an on-line least-squares fit. And, if the chosen orthogonal modes correspond to natural low-energy bending modes, as in the system designed for the European Southern Observatory New Technology Telescope (NTT), the calculated corrective forces will likely be of moderate size. Only the portion of the mirror surface distortions corresponding to the chosen set of modes will be corrected; the residual surface errors not well described by the modes will remain. However, for a zero-expansion thin meniscus mirror any figure changes will be caused by self weight or external forces, and are likely to take the form of the same low-energy bending modes.

The case of a structured borosilicate mirror is somewhat different. We anticipate much of the surface distortion will result from variations in the performance of the thermal control system. The figure changes caused by relative expansion of different parts of the mirror structure will not necessarily conform to low-energy bending modes of the mirror. It is possible that by employing modal precalculation, we would be accomplishing only part of the correction the system would be capable of producing. One alternative is to perform a least-squares fit in real time to find the forces that minimize the displacements at the 292 grid points on the mirror surface. As the price of computing power declines, affordable computers can now perform these calculations very rapidly.

Before the least-squares fit is performed tilt, focus and coma are subtracted from the surface data. It would be pointless to try to correct tilt (pointing) and focus with the forces on the back of the mirror, and coma is best corrected by aligning the secondary mirror.

One problem remains, what can be done if the calculated active forces are larger than the system can safely provide? A force that is too large cannot be truncated individually. To maintain static equilibrium and avoid image shifts, five constraints have been imposed on the least-squares fit. The summation of active forces in each of the three support zones must be zero, and the summation of moments exerted on the mirror must be zero in two coordinate directions. Reducing one force individually would violate these constraints. To scale back the entire set of forces by an equal ratio would satisfy the constraints, but could greatly reduce the amount of correction.

The approach we are using is to precalculate a force reduction vector for each actuator. This vector consists of a set of 66 forces that satisfies the following conditions: 1) there is a unit force at the actuator position in question, 2) the other 65 forces satisfy the five constraints, and 3) the resulting figure change has minimum RMS amplitude. Multiples of these force reduction vectors can be added to the solution vector to reduce out of bound forces to acceptable levels, with (by definition) minimum effect on the correction.

3. DESCRIPTION OF THE ACTIVE OPTICS SYSTEM

3.1 Mechanical hardware

The complete experimental assembly consists of the mirror, its mirror cell, and associated equipment attached to the cell including the mirror support, the active optics system, the thermal control system and the position and orientation control system.

The 3.5-meter mirror blank is shown in figure 2. The mirror has been polished to a spherical figure to facilitate testing from its center of curvature. It has also been coated with evaporated aluminum.

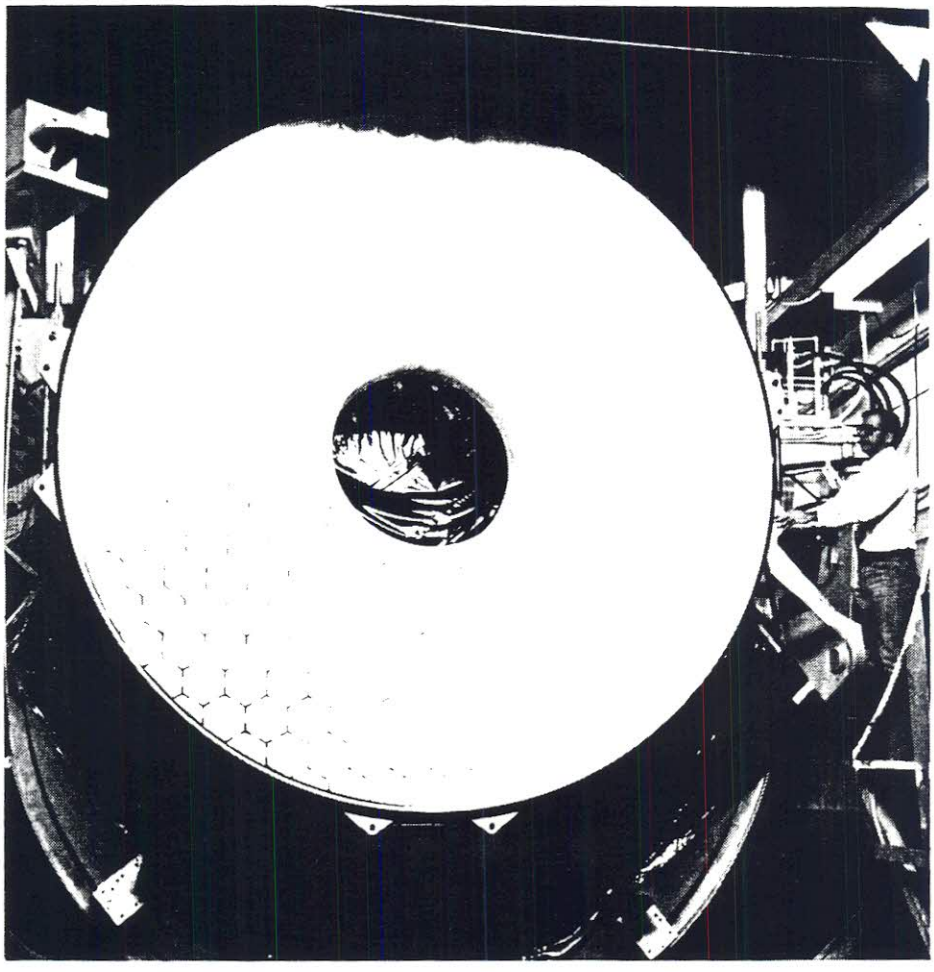

Figure 2. The 3.5-meter borosilicate mirror before it was aluminized.

The mirror support is designed to be completely passive, that is, the weight of the mirror is entirely supported by passive mechanisms. It is easy to confuse the support and active optics systems because both are combined in the same mechanical assemblies, but as mentioned above the active optics system carries no net weight.

The support system is designed to be astatic, that is, the correct forces are applied regardless of small positional changes between the mirror and cell. The axial support is configured as a three-zone hydraulic whiffletree. Each zone has 22 discrete support points, connected together hydraulically. Each support point is a hydraulic cylinder incorporating a flexible diaphragm (Bellofram®) to reduce friction and hysteresis. The cylinder is connected to the back of the mirror by a lightweight tubular column. A load cell in each column measures the force applied to the mirror. Four different diameters of cylinders are used, and the applied forces vary as the areas of the cylinders.

The lateral support is a system of 24 hydraulic lever mechanisms that contact the mirror at its back surface. Because the lateral forces do not act through the center of gravity of the mirror, static equilibrium requires reaction forces at the axial support positions. Corrective axial force components are also needed to minimize figure distortion. Auxiliary hydraulic cylinders are coupled to 64 of the 66 axial support mechanisms to provide the required corrective forces.

The position and tilt of the mirror can be adjusted by changing the fluid levels in the lateral support system and the three zones of the axial support. A pair of adjustable-length tangent arms are attached to the back of the mirror near its edge to prevent side to side motion or rotation about the optical axis.

Any high-bandwidth disturbances, for example gusts of wind pushing on the mirror, are reacted by the axial support. Because of the whiffletree design, all 66 support locations resist a wind gust instead of just three hard points.

The active optics mechanisms apply forces to the back of the mirror in the axial direction. Each mechanism can either push or pull on the mirror, and the available magnitude of force does not depend on elevation angle. The force is applied by a stepper motor that drives a ball screw mechanism to deflect a spring (see figure 3). Stepper motors are used to minimize the heat load dissipated by the mechanisms.

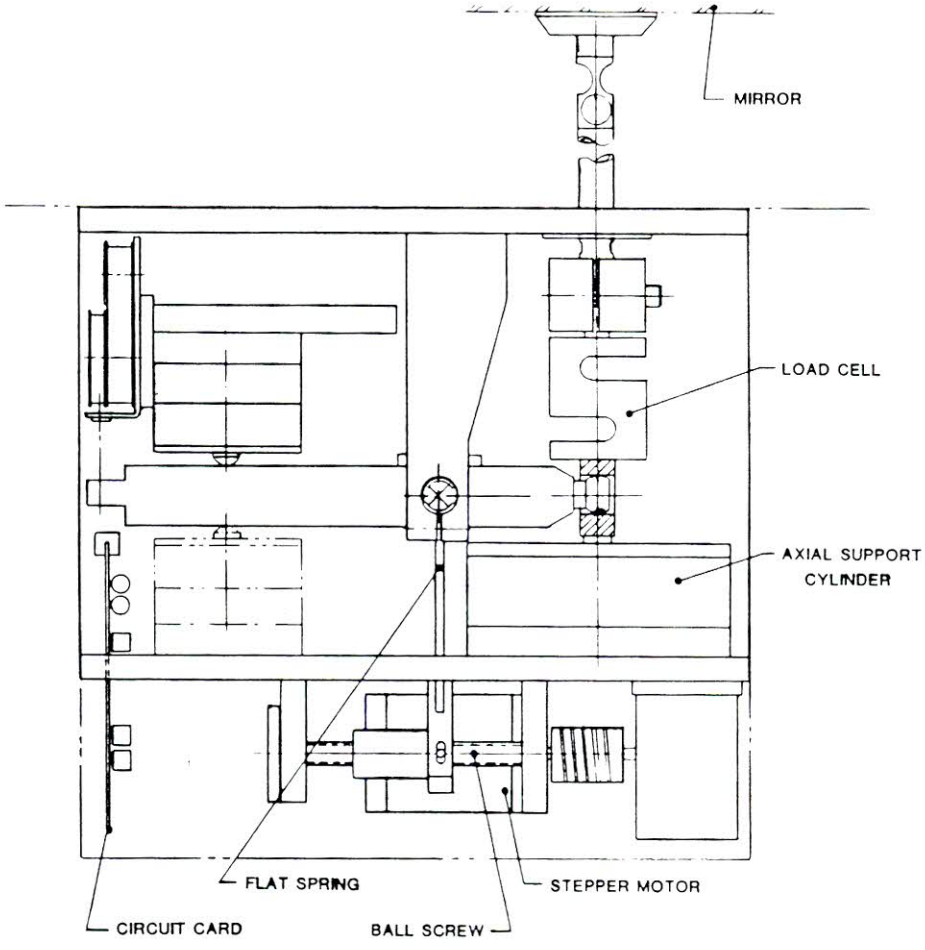

Figure 3. A diagram of one of the axial support/active optics mechanisms. The active force is produced by bending the flat spring, which couples to the mirror through a lever.

Each load cell has a rated capacity of ±1112 newtons (250 pounds). Limit switches in the mechanism restrict the magnitude of active force to this range, which is well within the safe force level for the mirror. Because the honeycomb mirror is relatively stiff, the active force range is approximately four times the average zenith-pointing axial support force. Preliminary tests indicate this full range is needed.

3.2 Control electronics

The active optics system is computer controlled. A circuit card in each actuator assembly reads the load cell, communicates with the central computer, and drives the stepper motor. The circuit cards were designed to be identical units, to facilitate maintenance.

Each circuit card contains a microprocessor and its associated RAM and EPROM chips. Communication with the host computer is through an RS-485 serial interface. An 8-bit binary identification code is hard-wired into the circuit card connector in each support mechanism. Whenever the system starts up this code is read and the location is identified.

The stepper motor controller/driver is a standard Kitt Peak circuit design. It applies chopped high voltage current pulses to the motor windings to increase the start-up torque. This circuit has been implemented using an SGS L298N IC driver and a custom programmable array logic (PAL) chip to generate the desired motor wave forms.

The load cell signal is conditioned by an Analog Devices AD 1B31 signal conditioner. The signal is then processed by a 12-bit analog-to-digital converter and the data is stored by the microprocessor, to be passed on to the host computer when requested. The force resolution is one-half newton (about two ounces).

4. DESCRIPTION OF THE EXPERIMENTAL SETUP

Testing of the active optics system is being done in the NOAO large optics polishing facility. A schematic diagram of this facility is shown in figure 4.

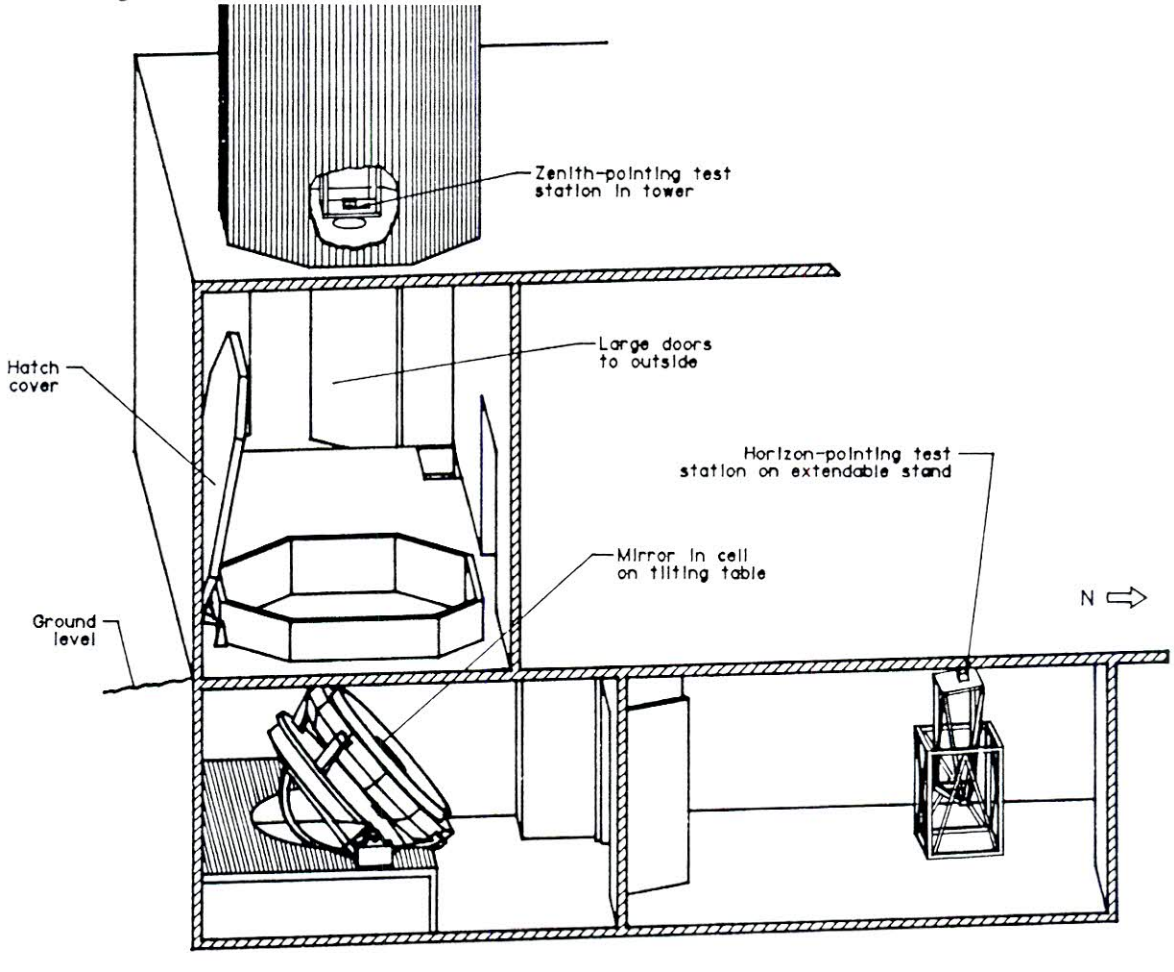

Figure 4. A schematic diagram of the NOAO large optics facility.

The mirror is installed in its mirror cell, mounted on the table of the 4-meter polishing machine, which can be tilted to allow the mirror to be tested from its center of curvature in zenith-pointing as well as horizon-pointing orientations (see figure 5). Optical test equipment can be located in a test tower above the polishing machine, as well as in the basement room directly in front of the polishing machine. At one end of this area, large doors can be opened to allow warm or cold outside air to blow into the room, creating a dynamically changing thermal environment.

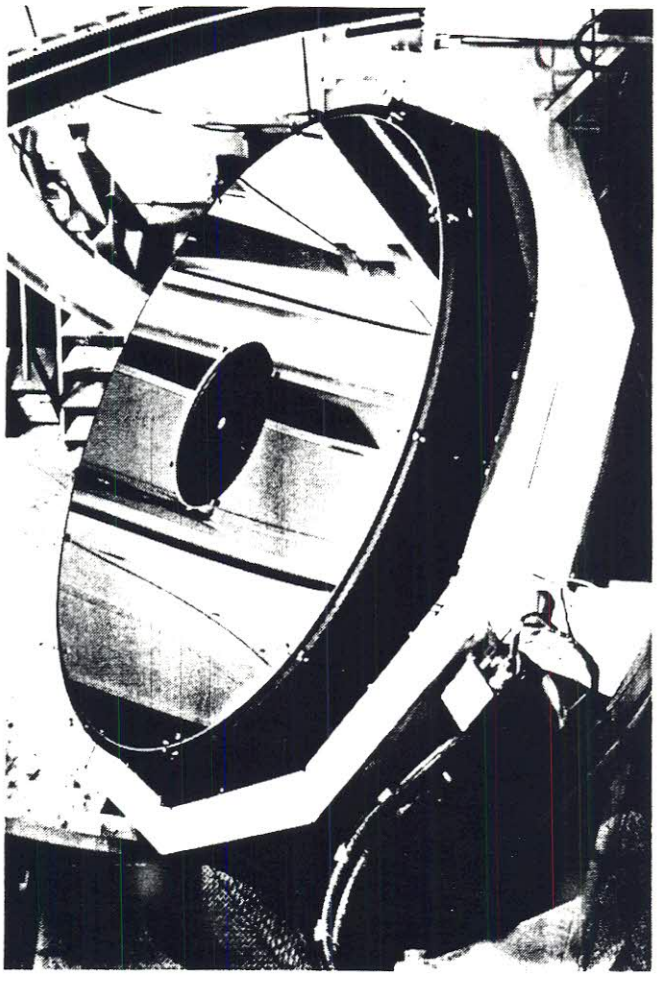

Figure 5. The 3.5-meter f/1.75 mirror mounted in its cell on the table of the 4-meter polishing machine.

5. PRELIMINARY TEST RESULTS

Testing of the active optics system has just begun. We are in the process of debugging control software, and will soon proceed with a full scale calibration of the system. A few preliminary exercises of the system have already been attempted, and while they have been of limited scope they give some indication of the potential the system will have when it is fully functional.

Figure 6 shows the results of the initial adjustment of the axial supports. The mirror had previously been tested on a hydraulic whiffletree polishing support, and had been figured to an accuracy of 42 nanometers RMS (figure 6A). After installation in the mirror cell the mirror was tested again. The axial support in the mirror cell is intended to apply identical forces to those applied by the polishing support, but it is a completely different mechanical design. We have also attached lateral supports and lateral defining arms to the mirror, and installed soft rubber gaskets at its inside and outside diameters.

When we adjusted the axial supports to their nominal force values and measured the mirror figure, it was distorted into the astigmatic surface shown in 6B. We are in the process of determining the source of the support errors that caused the figure change, but they will not cause a serious limitation to performance. After correction by the active optics system the mirror figure is better than it was on the polishing support, as shown in 6C.

6. CONCLUSIONS

It is still early in our test program, but we can already state two conclusions based on our preliminary results. First, we have demonstrated the 3.5-meter borosilicate honeycomb mirror is flexible enough to make effective use of an active optics system. And second, we have demonstrated that active optics is a very useful tool for compensation of unexpected errors in the mirror support system.

7. PLAN FOR FURTHER TESTING

Several months of additional testing is planned for the active optics system. The first procedure will be a complete empirical calibration. As described in section 2, finite-element analysis was used to predict the bending of the mirror, and Figures 6-10 show that good performance can be obtained simply using the finite-element results. It appears the influence functions must have approximately the calculated shape, although there is some indication their magnitudes may need to be scaled, since two or three iterations of the system were required to produce each of the patterns shown in Figures 7-10.

We anticipate that an experimental calibration of the system will lead to faster convergence and possibly better final results. The calibration will consist of the application of ±200 newton loads at each actuator in turn. The resulting influence functions will be measured by interferometer, and a new influence matrix will be prepared. From these measurements we will determine the difference between the actual stiffness of the mirror and the stiffness calculated by finite-element analysis. We will also be able to more accurately predict the response of the mirror to support force errors.

To verify the calibration of the system, we will produce more individual Zernike terms. Twenty-five low order terms will be attempted. Finite-element modeling indicates the system should be able to effectively produce some 15 of these terms.

The active optics system must be able to adjust support forces during an exposure, without introducing significant vibration and without moving the image. We will measure the stability of our system with an autocollimating microscope that places the image of an illuminated pinhole at the mirror center of curvature, and examines the stigmatic image formed by the mirror. A video camera will record any image motion that occurs during operation of the active optics system.

A key part of the active optics system will be the optical test equipment that provides feedback about the mirror figure. We plan to evaluate two types of feedback system, curvature sensing and Hartmann-Schack. The accuracy of each method will be checked by comparison to measurements made with the scatterplate interferometer.

The active optics system is currently based on mirror surface height information. It is also possible to directly use the slope information from the Hartmann-Schack test or curvature information from the curvature sensing test. The influence matrix could be set up in terms of slopes or curvatures instead of displacements. This might allow more direct computation of the corrections, without the need for integration. We plan to develop different versions of the control software to explore these possibilities.

We also hope to investigate another issue involving the control philosophy. As mentioned in section 2, we would like to know whether a system based on modal precalculation would work better than a system based on a real time least-squares fit. Therefore, we will set up both approaches in our control system, and then compare the figure correction accomplished with each.

Another question we will try to answer is to what extent the active optics system can correct mirror distortions caused by uneven temperatures. If uneven temperatures produce only low-spatial frequency aberrations that are easily corrected, a much looser error budget for thermal control could be allowed, which could reduce the cost of the telescope. We will perform a number of experiments in which we purposely introduce thermal gradients into the borosilicate mirror, and then attempt to eliminate the resulting deformations with active optics.

Other tests will be performed to help us evaluate practical factors such as cost, reliability, and compatibility with the telescope environment. When the testing program has been completed, the mirror will be refigured as an asphere and the active optics system will be rebuilt as needed to improve its performance, before the mirror and its cell are installed in the WIYN Telescope.

8. ACKNOWLEDGEMENTS

Many people have contributed to the work reported here. In particular we would like to thank Gary Poczulp for extensive help in getting the active optics hardware assembled and working, as well as for performance of the optical testing. We would also like to thank Earl Pearson for many valuable discussions of active optics theory, Bob Harris for mechanical design of all the hardware involved in the experiment, Ron Harris, Larry Junco, John Kapp, Morris Kaufman, Lee Macomber and Roger Repp for fabrication of the mechanical hardware, and Rose Andresen for fabrication of electronic hardware.

9. REFERENCES

1. L. Stepp, "3.5m Mirror Project at NOAO," *Advanced Technology Optical Telescopes IV*, ed. L. D. Barr, vol. 1236, pp. 615-627, SPIE, Tucson, 1990.

2. M. Johns and C. Pilachowski, "WIN 3.5-m Telescope Project," *Advanced Technology Optical Telescopes IV*, ed. L. D. Barr, vol. 1236, pp. 2-12, SPIE, Tucson, 1990.

3. J. H. Hardy, "Active optics--don't build a telescope without it!," *Advanced Technology Optical Telescopes*, ed. G. Burbidge and L. D. Barr, vol. 332, pp. 252-259, SPIE, Tucson, 1982.

4. R. N. Wilson and L. Noethe, "Mirrors and supports," *ESO Conference on Very Large Telescopes and Their Instrumentation*, ed. M.-H. Ulrich, Proc. No. 30, pp. 373-388, ESO, Garching, 1988.

5. E. Pearson, L. Stepp and J. Fox, "Active Optics Correction of thermal distortion of a 1.8-meter mirror," *Opt. Eng.*, vol. 27 No. 2, pp. 115-122, 1988.

6. R. N. Wilson, F. Franza and L. Noethe, "Active optics I. A system for optimizing the optical quality and reducing the costs of large telescopes," *Journal of Modern Optics*, Vol. 34 No. 4, pp. 485-509, 1987.

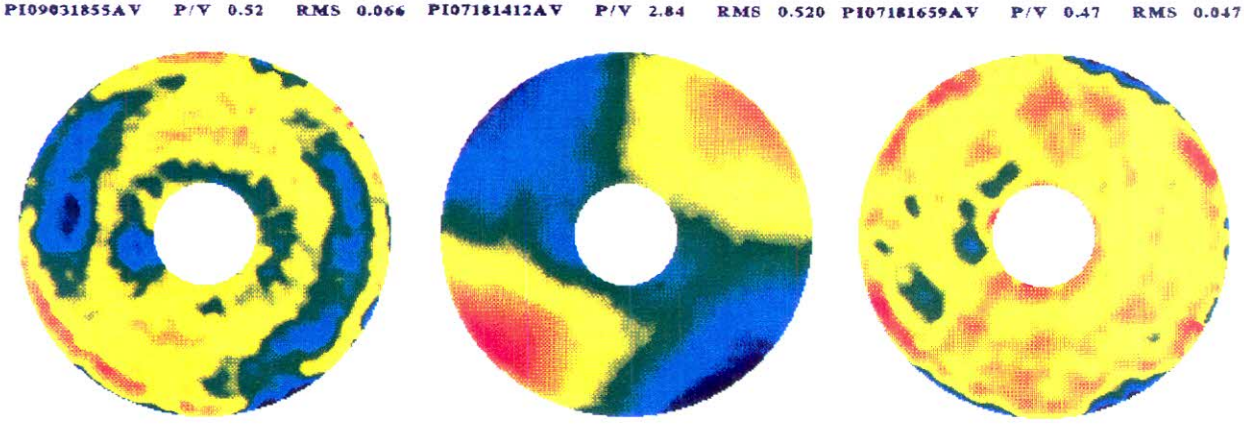

Figure 6A. A phase map showing the mirror figure measured by scatterplate interferometer at the conclusion of the polishing operation.

Figure 6B. A phase map showing the mirror figure when first tested on its full support system in the mirror cell.

Figure 6C. A phase map showing the mirror figure after correction with the active optics system. Note the figure improvement compared to the original polished surface.

Part of our testing program is to exercise the active optics system by distorting the mirror into different Zernike terms. Figures 7 through 10 show initial attempts at several low-order terms. In each case, the mathematical term serving as the goal is on the left and the measured change in mirror figure is on the right. In the equations, the surface deformation w is in wavelengths, λ = 0.6328 microns, and the radius r is normalized to equal 1.0 at the outer edge of the aperture. The peak-to-valley (PV) and RMS figure amplitudes are also shown in units of wavelengths.

The mirror is able to produce these Zernike terms quite well, except for high slope areas around the outer edge of the pattern.

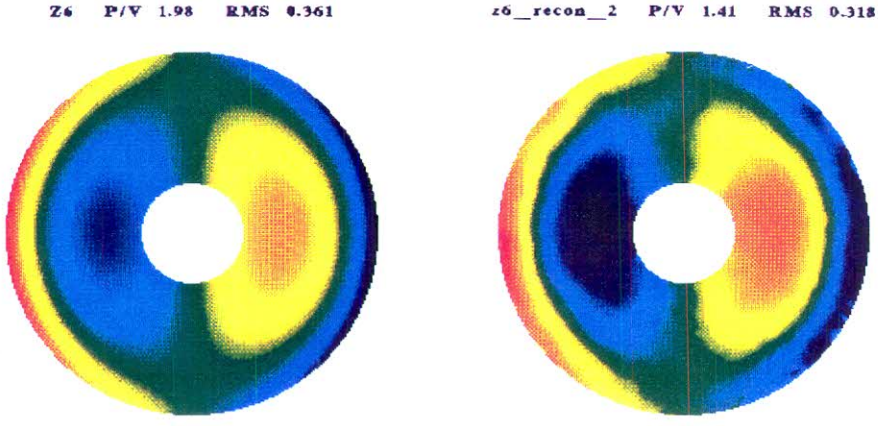

Figure 7. Experimental production of a Zernike term corresponding to coma: $w = (3r^3 - 2r)\cos\theta$.

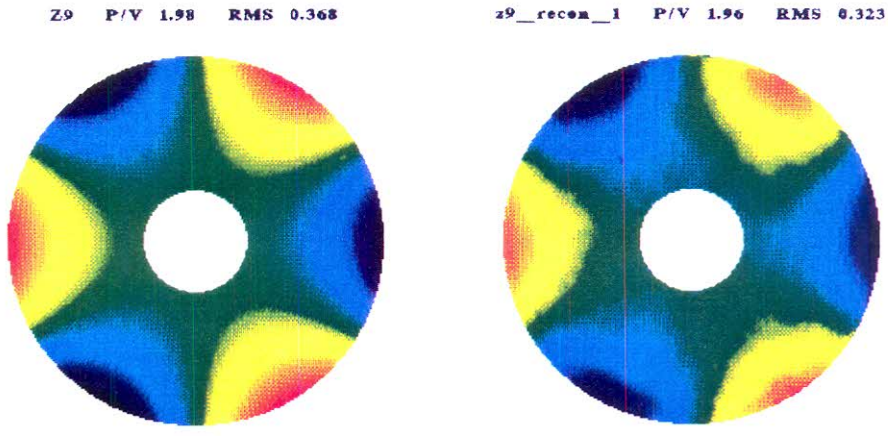

Figure 8. Experimental production of a Zernike term corresponding to trefoil: $w = r^3 cos\,3\theta$

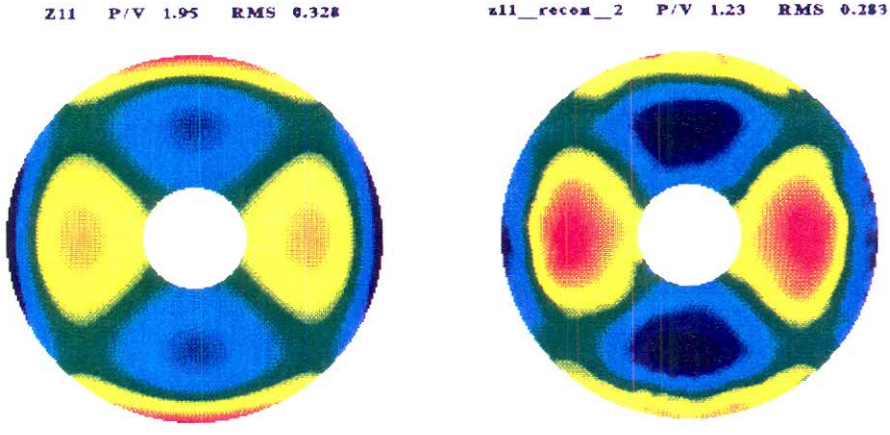

Figure 9. Experimental production of the Zernike term: $w = (4r^4 - 3r^2)cos\,2\theta$

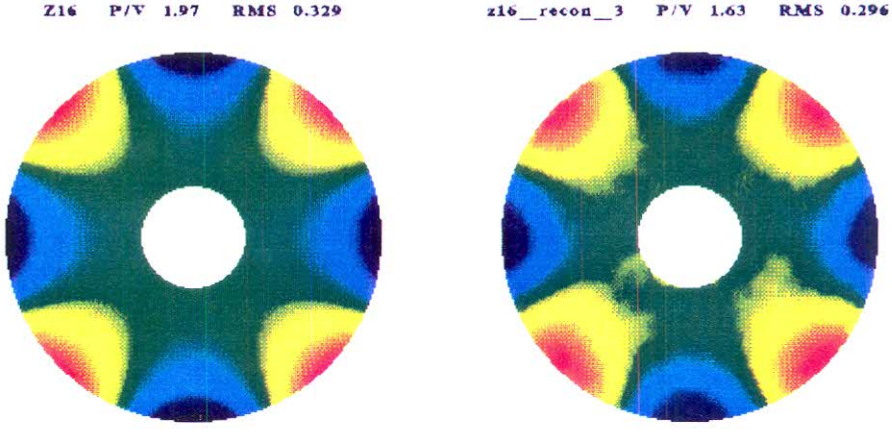

Figure 10. Experimental production of a Zernike term corresponding to quatrefoil: $w = r^4 cos\,4\theta$